Analyst

Accepted Manuscript

ROYAL SOCIETY OF CHEMISTRY

www.rsc.org/analyst

Cite this: DOI: 10.1039/c0xx00000x

www.rsc.org/xxxxxx

ARTICLE TYPE

Old is New Again: a Chemical Probe for Targeting Mitochondria and Monitoring Mitochondrial Membrane Potential in Cells

Lu Zhang,[a,d] Wenwen Liu,[a,d] Xianhong Huang,[b] Guanxin Zhang,[b] Xuefei Wang,[c] Zhuo Wang,*[a] Deqing Zhang,*[b] and Xingyu Jiang*[a]

Received (in XXX, XXX) Xth XXXXXXXXX 20XX, Accepted Xth XXXXXXXXX 20XX

DOI: 10.1039/b000000x

Here, we explore the new application of an old molecule. We find that the tetraphenylethene-indolium molecule (TPE-indo) can both image the mitochondria (in the aggregated state), and indicate mitochondria activity by the fluorescence change of TPE-indo. TPE-indo shows good photostability, longer emission wavelength, targeting effect for mitochondria, and better response to the changes of the mitochondrial membrane potential (ΔΨm).

Molecules with aggregation-induced emission (AIE) characteristics are non-fluorescent when dispersed, but show strong fluorescence in the aggregated state, and exhibit good photostability than the traditional fluorescent molecules. [1] Due to their superior characteristics, molecules with AIE feature are widely used in biochemical analysis.[2] Tetraphenylethene (TPE) derivatives, which have AIE feature, can stain living cells and microbes on the basis of good optical characters and convenient synthesis procedure.[3] Recently, TPE derivatives are reported to be able to track mitochondria in cells on the basis of the target function of triphenylphosphonium (TPP).[4] Mitochondria are membrane-enclosed organelles found in most eukaryotic cells and play a major role in the generation of ATP and reactive oxygen species (ROS).[5] As an important physiologic mitochondrial parameter, ΔΨm (mitochondrial membrane potential) indicates the health and injury of a cell. [6] Researchers synthesize new probes for targeting mitochondria, learn its physiological function, and hope to indicate the relationship of health and disease. The fluorescent dyes for imaging mitochondria and measuring ΔΨm have been explored and used in biological field.[7] Most of the mitochondrial dyes are typically lipophilic cationic compounds that equilibrate across membranes in a Nernstian fashion. These dyes accumulate into the mitochondrial membrane matrix space in inverse proportion to ΔΨm, such as TMRM (tetramethylrhodamine methyl ester), TMRE (tetramethylrhodamine ethyl ester), Rhodamine 123 (Rhod123), and JC-1. The existing probes have some defects, such as, high cytotoxicity, limited selectivity, and poor photostability, so we are still on the way to require better probes for targeting mitochondria. The reported TPE-TPP probes can light up the mitochondria in cells, but cannot measure the change of ΔΨm.[4] The specific targeting mainly due to the electrostatic interaction of TPP and the mitochondrial membrane. However, when ΔΨm changes, the fluorescence of TPE-TPP probe does not change, [4a] which infers the electrostatic interaction between TPP and membrane still exists. Thus we want to find a new probe to image mitochondria and monitor the change of ΔΨm simultaneously. On the basis of most mitochondrial probes have positive charge groups, (eg. Rhd123, TMRM, TMRE, JC-1, MitoTracker) we chose indolium positively-charged moiety for targeting and synthesised the tetraphenylethene-indolium molecule (TPE-indo). We find TPE-indo can go into the bacteria and show strong fluorescence. [8] It is known that bacteria and mitochondria share the evolutionary origin, and they both have strong negative cellular potential. [6c] So we suggest that TPE-indo can be a good candidate as a mitochondrial probe.

The surface electrostatic potential maybe a key factor, and affects the interaction between a probe and mitochondria. We calculated and compared the electrostatic potential of TPE-TPP and TPE-indo by Gaussian 09, and the results showed the isosurface of TPP is more positive than indolium group. The weaker interaction between the probe and the mitochondrial membrane may make a different function. Thus we put TPE-indo in the living cells and observed different behaviours compared with TPP probes. TPE-indo can accumulate in the negatively charged mitochondria, and monitor ΔΨm by the changes of fluorescence, which is the first time to be reported.

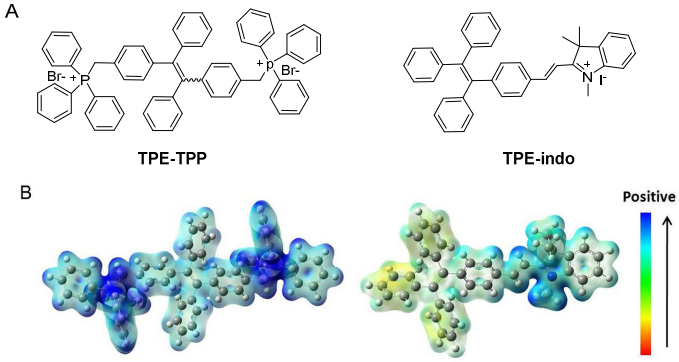

Figure1. TPE-TPP and TPE-indo. (A) Chemical structure of TPE-TPP and TPE-indo. (B) Positive isosurfaces (deep blue means more positive) of the electrostatic potential of TPE-TPP and TPE-indo. Calculated by Gaussian 09 program.

As a biological probe, the cytotoxicity determines its application. The cytotoxicity of TPE-indo is evaluated using Cell Counting Kit-8 (CCK-8) and cervical cancer HeLa cells.[9] The cell viability value almost keeps about 1, which indicates that cells have good status with different concentrations of TEP-indo. Even the concentration of TPE-indo is as high as 50 μM, neither the viability nor the morphology of HeLa cells is significantly affected after 24 hours of incubation (Figure S1).

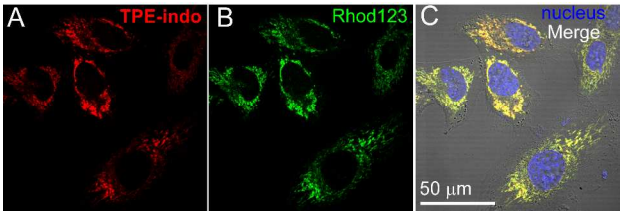

Figure2. TPE-indo molecules target mitochondria. (A) Fluorescent image of HeLa cells stained with TPE-indo (20 μM, red). (B) Fluorescent image of HeLa cells stained with Rhod123 (20 μM, green). (C) Merged image of TPE-indo, Rhod123, cell morphology (bright field), and nucleus stained by Hoechst 33342 (blue). Colocalization of TPE-indo and Rhod123 makes the fluorescence become yellow. Excitation wavelengths of Hoechst 3342, Rhod123, and TPE-indo are 405 nm, 514 nm, and 543 nm, respectively.

TPE-indo passes the cytotoxicity test favorably, and it is used to stain the cells. To assess the capacity of TPE-indo for staining cells, HeLa cells are incubated with the TPE-indo solution (20 μM) for 20 minutes. The excitation and emission maximum of TPE-indo in cells are detected by laser scanning confocal microscope (LSM--710, Zeiss), which are 543 nm and 569 nm (Figure S2). Compared with the previously described AIE probes for mitochondria,[4] the wavelength of the excitation of TPE-indo in cells is much longer, which increases the penetration depth and cell viability. As shown in Figure 2, TPE-indo colocalizes with Rhod123, a commercial mitochondrial dye with a high Pearson's correlation of 0.86. The amplified fluorescent image of HeLa cells stained with TPE-indo and Rhod123 with higher resolution is shown in Figure S3. The colocalization of TPE-indo and Rhod123 indicates that TPE-indo may at the same sub-mitochondrial location as Rhod123, which accumulates in the mitochondrial matrix after staining. [10]The colocalization of TPE-indo with the other commercial mitochondrial dye, MitoTracker, also shows good result. (Figure S4) In order to confirm the special mitochondrial targeting of TPE-indo, the distribution of TPE-indo in cells is further demonstrated by its colocalization with the immunofluorescence of ATP5B (Figure S4). ATP5B is a component in mitochondrial membrane that is related with the synthesis of ATP (adenosine-triphosphate). The immunofluorescence of ATP5B co-localize with the fluorescence of TPE-indo, which verify the mitochondrial targeting function of TPE-indo in cells further. In contrast to commercially available mitochondrial dye, **TPE-indo** does not require washing due to AIE feature and extremely low cytotoxicity (Figure S5). No washing step makes the staining process more convenient and economical.

To further show the superiority of **TPE-indo** as an ideal mitochondrial dye, we characterized its photostability by continuous laser irradiation. In order to get the real-time images, we used the laser of confocal microscope with power of 70 μW. We analyzed the fluorescent intensities of **TPE-indo** (543 nm,), JC-1 (543 nm), MitoTracker (543 nm), and Rhod123-stained cells (514 nm) in the range of 0-300 bleaching times (1.0 second /bleaching time) with the laser irradiation. The fluorescent intensity of TPE-indo almost does not decay for 300 bleaching times, while the fluorescent intensities of Rhod123 and JC-1 decay obviously after 100 bleaching times. (Figure 3A) The signal loss of **TPE-indo** is less than 10% after 300 bleaching times. In contrast, fluorescent signal of JC-1 is almost totally quenched and the other two dyes (Rhod123, MitoTracker) lost ~80% within 100 bleaching times. From the images of stained cells, we can also see the photo bleaching of these dyes in cells clearly. (Figure 3B) We think the anti-bleaching property of TPE-indo comes from the different emission mechanism of AIE.[1]

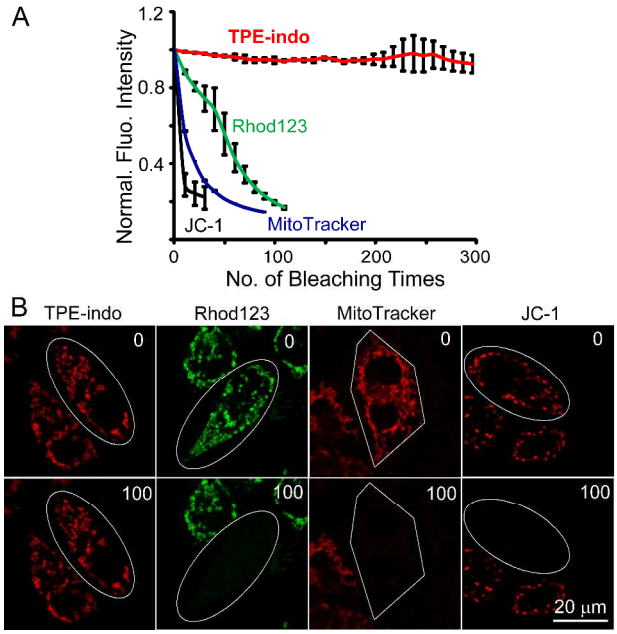

Figure 3. Superior photostability of TPE-indo. A) Signal loss of fluorescent emission with the increasing number of bleaching. B) Fluorescent images of HeLa cells stained with TPE-indo, Rhod123, MitoTracker, and JC-1 at 0 and 100 bleaching times respectively. The irradiation time is 1.0 s/bleaching.

As mitochondria are energy power-plants of cells, mitochondrial membrane potential (ΔΨm) relates to cells' capacity of generating ATP by oxidative phosphorylation and the change of ΔΨm is a key indicator of mitochondrial function.[6b,6c] However, not all the mitochondrial probes can monitor the change of ΔΨm. JC-1 can do this, while MitoTracker Green FM cannot. We compared the performance of TPE-indo and JC-1 on the application of ΔΨm monitoring with MitoTracker Green FM as a control. MitoTracher Green FM is a mitochondrial dys that cannot indicate the change of ΔΨm. Both TPE-indo and JC-1 pre-stained HeLa cells are incubated with valinomycin, which is a kind of ΔΨm inhibitor,[11] on the microscope for 20 minutes to detect the attenuation of fluorescence. The cells show decreased fluorescent intensity (Figure 4A). Compared with Mitotracker Green FM and JC-1, the response of TPE-indo stained cells are more sensitive to the same decrease of ΔΨm (Figure 4B). It is reported that the decrease of ΔΨm relates with the cell apoptosis,[6b] thus we infer that TPE-indo may be able to indicate the apoptosis of living cells. In order to confirm our suggestion, we treated HeLa cells with H_2O_2, which can cause apoptosis of cells. The untreated HeLa cells and H_2O_2-treated cells are stained by TPE-indo (20 μM), and the fluorescent intensities are analyzed by the flow cytometry. The fluorescent intensity of H_2O_2-treated cells at 564-600 nm decreased by 52.5% compared with normal cells (Figure 4C). These results confirm that TPE-indo can be used as a probe for cell apoptosis based on its capability of monitoring ΔΨm.

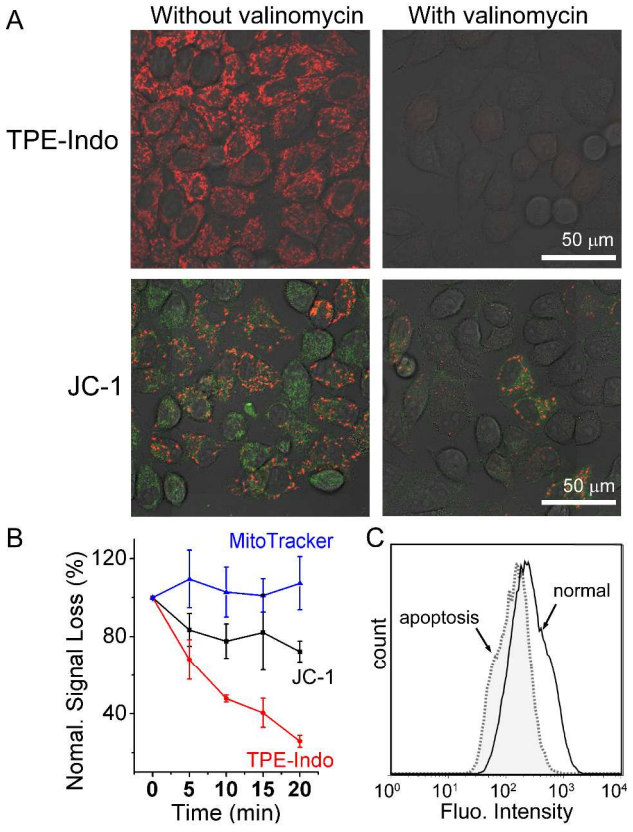

Figure 4. TPE-indo monitors the change of ΔΨm. A) TPE-indo (Top) and JC-1 (Bottom) stained HeLa cells (left) and valinomycin-treated HeLa cells (right). B) The time-dependent response of fluorescent signal of TPE-indo, JC-1 and MitoTracker Green FM with the decrease of ΔΨm. C) H_2O_2-treated HeLa cells show decreased fluorescent intensity (dotted line) of TPE-indo compared with normal cells (full line) in the flow cytometry analysis.

The reason that TPE-indo can aggregate in mitochondria and show response to the change of ΔΨm is due to the positive electrostatic surface of TPE-indo. With the positive charged indolium moiety, TPE-indo molecules accumulate in both cytoplasm and mitochondria driven by their electrical potential (Ψm) based on electrostatic interaction. As mitochondrial ΔΨm ranges -140~-180 mV in most normal cells, the concentration of TPE-indo molecules accumulated in mitochondria can be several hundred-fold higher than that in cytoplasm[6c, 12]. Thus, emission of TPE-indo in mitochondria is enhanced according to its AIE property. It is also reported that the viscosity and protein content of the mitochondria are 7~8 times and 5 times of that in cytoplasm, respectively.[13] Therefore, we wonder if the higher viscosity and protein content can enhance the fluorescence of TPE-indo in mitochondria. By using glycerol to adjust the viscosity of the solution, we increase the solution viscosity from 1.0 mPa•s to 1412 mPa•s and fixed the concentration of TPE-indo at 5 μM. Upon increasing the viscosity, the emission intensity of TPE-indo is enhanced dramatically. Through the adding of BSA into glycerol solution to increase the protein content from 10 mg/mL to 90 mg/mL, the emission intensity of TPE-indo is enhanced further (Figure S6). This is indeed consistent with its fluorescence spectra in cells measured by the confocal microscope. We also investigated the spectra of TPE-indo in the solvents with different pHs and polarities. We recorded the fluorescence of TPE-indo from pH 2 to pH 10 in aqueous solution. Although different pHs induce the change of fluorescence, the intensities are pretty lower than that in the viscous solution. In order to test the polarity effect, we used four solvents (water, acetonitrile, methanol, and acetone) with different polarities to dissolve TPE-indo, and recorded the emission spectra. The polarities of acetonitrile, methanol and acetone are smaller than water, and can induce part aggregation of TPE-indo with the increased fluorescence. But, the intensities are much lower than that in the glycerol. (Figure S7) So pH and polarity can affect the fluorescence of TPE-indo in some degree. However, the fluorescent change is much smaller compared with the effect of viscosity and protein. The high viscosity and protein content in mitochondria mainly cause the aggregation of TPE-indo molecules and enhance the fluorescence of TPE-indo further. As we demonstrated above that the uptake of TPE-indo molecules is related to ΔΨm, and the ΔΨm of cancerous cells is higher than non-cancerous cells.[14] We suggest that TPE-indo may have different response to different cells. We apply the flow cytometry to screen different kinds of cells cultured with TPE-indo. The average fluorescent intensities of TPE-indo, both in human and mouse cells, are higher in cancerous cells than that in non-cancerous cells. For the cells from human source, Table 1 shows the fluorescent intensities of the cancerous cells (HeLa and MCF-7) are higher than non-cancerous cells (HUVEC cells). In the mouse cells, the fluorescence intensity of the cancerous cell (4T1) is higher than the other two kinds of non-cancerous cells (MC3T3 and NIH3T3). Compared with the human cells, TPE-indo shows weaker fluorescence in mouse cells. These results indicate the potential application of TPE-indo in the imaging of cancerous cell, because cancerous cells uptake more probes compared with normal cells. In the further work, we plan to integrative some targeting groups with TPE-indo for imaging cancerous cells *in vivo*.

Table 1. Fluorescent intensity of TPE-indo stained different types of cells analyzed by flow cytometry.

Cell name[a]	Source	Cancerous cells	Fluo. Intensity
HeLa	Human	Yes	427.97
MCF-7	Human	Yes	390.89
HUVEC	Human	No	294.70
4T1	Mouse	Yes	47.04
MC3T3	Mouse	No	12.11
NIH3T3	Mouse	No	6.45

[a] HeLa: human cervical cancer cells; MCF-7: human breast cancer cells; HUVEC: human umbilical vein endothelial cells; 4T1: mouse breast cancer cells; MC3T3: mouse osteoblast cells; NIH3T3: Mouse fabroblast cells.

Conclusions

The structure of TPE-indo with an aggregation-induced fluorophore and a positively-charged indolium endows its capability of mitochondrial imaging and monitoring ΔΨm. We demonstrate its specificity to mitochondria in cells, its excellent photostability and low cytotoxicity by the comparison with

commercial mitochondrial dyes. We calculate the surface electrostatic potential of TPE-indo to try to understand its targeting behaviour. We further reveal that the higher viscosity and protein concentration in mitochondria can enhance and change the emission of TPE-indo molecules, which is another mainly effect to explain the targeting of TPE-indo. TPE-indo can monitor the change of $\Delta\Psi m$, which is first time to find this function in AIE mitochondrial probes. We also find that TPE-indo shows the higher selectivity for the mitochondria of cancer cells, and will do research for further development of AIE-based bioprobes. This is an old molecule, but it has a totally new property and application here. When we open a new window, we will see different scenery.

Experimental Section

Cell culture. Cells were cultured with Dulbecco's modified Eagle's medium (DMEM; Gibco) supplemented with fetal bovine serum (FBS, 10%; Gibco), Penicillin&Streptomycin (1%), Glutamine (1%), and maintained in CO_2 (5%) at 37°C.

Cell viability. Viability of cells was assayed by Cell Counting Kit-8 (CCK-8) with the absorbance of 450 nm being detected using a plate reader (Tecan infinite M200). HeLa cells grew overnight on 96-well culture plate (10, 000 cells per well). TPE-indo with various concentrations was added in the 96-well plate. After 24 hours incubation, cells were washed by culture medium and 10 μl of CCK was added to each well (containing 90 μl of medium). After 2 hours of incubation, the optical density at 450 nm was read by plate reader (Teican).

Cell Imaging. The live cells were stained with TPE-indo, JC-1 (5 ug/ml), MitoTracker (200 nM), Rhod123 (20 μM), and Hoechst 33342 (1:10000) for different requirement. The cells were imaged by a confocal microscope (Zeiss LSM710) and the power of the laser is lower than 10 μW.

Spectrum analysis of TPE-indo in cells was taken by confocal microscope (Zeiss, LSM710) under lambda mode with excitation wavelength of 543 nm. The fluorescent images were acquired under each 10 nm in the wavelength range of 549 – 659 nm. For the photostability test, cells were imaged by a confocal microscope (Zeiss, LSM710). TPE-indo, MitoTracker, and JC-1 were excited by 543 nm (70 μW). Rhodamine 123 was excited by 514 nm (80 μW).

For irradiation experiment, the stained cells without washing TPE-indo in culture medium were irradiated by the laser (488 nm, 543 nm, 100 μW) of confocal microscope 100 times as a cycle for 30 min and images were taken once every cycle.

Cell imaging with valinomycin. For valinomycin treatment, the stained cells were then incubated with 200 ng/mL valinomycin. Images were then captured by confocal microscope from 0 min to 20 min with 5 min intervals.

Immunostaining. For immunostaining, cells were washed by phosphate-buffered saline twice, and fixed with 4% paraformaldehyde solution for 30 minutes. Cells were washed three times by PBS for 5 minutes each, and permeabilized with 0.3% Triton X-100 for 10 minutes. 10% goat serum solution was used to block nonspecific binding for 1 hour. Primary antibodies (anti-ATP5B, gift from Prof. Jane Ying Wu's lab) were incubated over night at 4°C and secondary antibodies (Alexa Fluor 488 goat anti- rabbit IgG, Invitrogen) were incubated for 1 hour at room temperature.

Flow cytometry analysis. For apoptosis detection, control and H_2O_2–treated HeLa cells (2 mM, 30 min) were harvested and processed for the apoptosis staining using the Annexin V Apoptosis Detection Kit FITC (eBioscience). For each experiment, 20,000 cells were analyzed using a BD FACS Calibur flow cytometer (Becton Dickinson) and FlowJo software (TreeStar, Inc).

Viscosity experiment. Glycerol, and bovine serum albumin (BSA) were used to adjust the viscosity and protein content of solution. For viscosity experiment, the constant concentration of TPE-indo is 5 μM and the content of glycerol increased from 10% to 100 % (v/v) in water solution. The solution was excited at 450 nm and the fluorescence spectra were recorded by on a Hitachi F-4500 spectrophotometer at 25°C. For protein experiment, BSA was added to the glycerol/water solution (65%, v/v) of TPE-indo (5 μM). As the increase of BSA content from 10 mg/mL to 90 mg/mL, the solution was excited at 450 nm and the fluorescent spectra were recorded by on a Hitachi F-4500 spectrophotometer at 25°C.

pH and polarity experiments. For pH and polarity experiments, the constant concentration of TPE-indo was 5 μM. Buffers with pH of 2, 3, 4, 5, 6, 7, 8 were prepared by regulating the proportion of disodium hydrogen phosphate and citric acid. Sodium hydroxide was used to adjust pH of buffers from 8 to 9 and 10. Water, methanol, acetonitrileand and acetone were used to study the fluorescence of TPE-indo dissolved in solutions with various polarity.

Theoretical Calculation. The calculation of the electrostatic potential is performed with the Gaussian 09. The formatted checkpoint file is used as input in which the nuclear positions and charges, the parameters of the basis set, and the density matrix elements are specified.

Acknowledgements ((optional))

This research was supported by National Natural Science Foundation of China (21222502, 91213305), the Ministry of Science and Technology (2011CB933201), Youth Innovation Promotion Association (CAS), the CAS/SAFEA International Partnership Program for Creative Research Teams, the "Strategic Priority Research Program" of the Chinese Academy of Sciences, Grant No.XDA09030305, National High Technology Research and Development Program of China (2012AA022703).

Notes and references

[a] *L. Zhang, Dr. W. W. Liu, Prof. Z. Wang, and Prof. X. Y. Jiang, Beijing Engineering Research Center for BioNanotechnology & CAS Key Lab for Biological Effects of Nanomaterials and Nanosafety, National Center for NanoScience and Technology, No.11 ZhongGuanCun BeiYiTiao, 100190 Beijing, China. Fax: (+) 86 10 8254 5631 E-mail: xingyujiang@nanoctr.cn, wangz@nanoctr.cn*

[b] *X. H. Huang, Prof. G. X. Zhang, and Prof. D. Q. Zhang Beijing National Laboratory for Molecular Science, Organic Solids Laboratory, Institute of Chemistry, Chinese Academy of Science, Zhongguancun North First Street 2, 100190. Beijing, China. E-mail: dqzhang@iccas.ac.cn*

[c] *School of Chemistry and Chemical Engineering, University of Chinese Academy of Sciences, Beijing 100049, China*

[d] *These authors contributed equally to this work.*

† Electronic Supplementary Information (ESI) available: [details of any supplementary information available should be included here]. See DOI: 10.1039/b000000x/

1 a) Y. N. Hong, J. W. Y. Lam, B. Z. Tang, *Chem. Soc. Rev.* 2011, **40,** 5361-5388; b) R. R. Hu, N. L. C. Leung, B. Z. Tang, *Chem. Soc. Rev.* 2014, **43,** 4494-4562.

2 a) K. Cui, Z. L. Chen, Z. Wang, G. X. Zhang, D. Q. Zhang, *Analyst* 2011, **136**, 191-195; b) X. Xu, J. Huang, J. Li, J. Yan, J. Qin, Z. Li, *Chem. Commun.* 2011, **47**, 12385-12387; c) X. Shen, G. X. Zhang, D. Q. Zhang, *Org. Lett.* 2012, **14**, 1744-1747; d) Y. Y. Liu, Z. Wang, G. X. Zhang, W. Zhang, D. Q. Zhang, X. Y. Jiang, *Analyst* 2012, **137**, 4654-4657; e) H. B. Shi, R. T. K. Kwok, J. Z. Liu, B. G. Xing, B. Z. Tang, B. Liu, *J. Am. Chem. Soc.* 2012, **134**, 17972-17981; f) N. Zhao, M. Li, Y. L. Yan, J. W. Y. Lam, Y. L. Zhang, Y. S. Zhao, K. S. Wong, B. Z. Tang, *J. Mater. Chem. C* 2013, **1**, 4640-4646; g) Y. Y. Yuan, R. T. K. Kwok, G. X. Feng, J. Liang, J. L. Geng, B. Tang, B. Liu, *Chem. Commun.* 2014, **50**, 295-297; h) L.R. Xu, Y. Li, S. H. Li, R.R. Hu, A. J. Qin, B. Z. Tang, B. Su, *Analyst* 2014,**139**, 2332-2335;

3 a) M. Faisal, Y. Hong, J. Liu, Y.Yu, J. W. Y. Lam, A. Qin, P. Lu, B. Z. Tang, J. *Chem. Eur. J.* 2010, **16**, 4266-4272; b) D. Ding, K. Li, B. Liu, B. Z. Tang, *Accounts. Chem. Res.* 2013, **46**, 2441-2453; c) J. Mei, Y. Wang, J. Tong, J. Wang, A. Qin, J. Z. Sun, B. Z. Tang, Chem. Eur. J. 2013, **19**, 613-620; d) Y. Huang, F. Hu, R. Zhao, G. Zhang, H. Yang, D. Zhang, *Chem. Eur. J.*, 2014, **20**, 158-164.

4 a) C. W. T. Leung, Y. Hong, S. Chen, E. Zhao, J. W. Y. Lam, B. Z. Tang, *J. Am. Chem. Soc.* 2013, **135,** 62-65; b) Q. Hu, M. Gao, G. Feng, B. Liu, *Angew. Chem. Int. Ed.* 2014, **53**, 14225 –14229.

5 a) L. A. Sena, N. S. Chandel, *Mol. Cell* 2012, **48**, 158-167; b) F. Liu, T. Wu, J. F. Cao, H. Zhang, M. Hu, S. G. Sun, F. L. Song, J. L. Fan, J. Y. Wang, X. J. Peng, *Analyst*, 2013, **138**, 775-778.

6 a) E. J. Griffiths, *Cardiovasc. Res.* 2000, **46**, 24-27; b) E. Gottlieb, S. M. Armour, M. H. Harris, C. B. Thompson, *Cell Death Differ.* 2003, **10**, 709-717; c) S. R. Jean, D. V. Tulumello, S. P. Wisnovsky, E. K. Lei, M. P. Pereira, S. O. Kelley, *ACS Chem. Biol.* 2014, **9**, 323-333.

7 a) S. Lee, X. Y. Chen, *ChemBioChem* 2011, **12**, 2120-2121; b) A. Mathur, Y. Hong, B. K. Kemp, A. A. Barrientos, J. D. Erusalimsky, *Cardiovasc. Res.* 2000, **46**, 126-138; c) D. Morisaki, H. S. Kim, H. Inoue, H. Terauchi, S. Kuge, A. Naganuma, Y. Wataya, H. Tokuyama, M. Ihara, K. Takasu, *Chem. Sci.* 2010, **1**, 206-209; d) S. W. Perry, J. P. Norman, J. Barbieri, E. B. Brown, H. A. Gelbard, *Biotechniques* 2011, **50**, 98-115; e) H. S. Yuan, H. Cho, H. H. Chen, M. Panagia, D. E. Sosnovik, L. Josephson, *Chem. Commun.* 2013, **49**, 10361-10363.

8 a) W. Chen, Q. Li, W. Zheng, H. Fang, G. Zhang, Z. Wang, D. Zhang, X. Jiang, *Angew. Chem. Int. Ed.* 2014, **53**, 13734-13739; b) X. Huang, X. Gu, G. Zhang, D. Zhang, *Chem. Commun.* 2012, **48**, 12195-12197.

9 a) Z. L. Chen, Y. Li, W. W. Liu, D. Z. Zhang, Y. Y. Zhao, B. Yuan, X. Y. Jiang, *Angew. Chem. Int. Ed.* 2009, **48**, 8303-8305; b) Y. Li, B. Yuan, H. Ji, D. Han, S. Q. Chen, F. Tian, X. Y. Jiang, *Angew. Chem. Int. Ed.* 2007, **46**, 1094-1096; c) Y. Zhao, Z. Chen, Y. Chen, J. Xu, J. Li, X. Jiang, *J. Am. Chem. Soc.* 2013, **135**, 12940-12943; d) Y. Y. Zhao, Y. Tian, Y. Cui, W. W. Liu, W. S. Ma, X. Y. Jiang, *J. Am. Chem. Soc.* 2010, **132**, 12349-12356.

10 R. C. Scaduto, Jr., L. W. Grotyohann, *Biophysical Journal* 1999, **76**, 469–477.

11 I. J. Furlong, C. L. Mediavilla, R. Ascaso, A. L. Rivas, M. K. L. Collins, *Cell Death Differ.* 1998, **5**, 214-221.

12 M. F. Ross, G. F. Kelso, F. H. Blaikie, A. M. James, H. M. Cocheme, A. Filipovska, T. Da Ros, T. R. Hurd, R. A. J. Smith, M. P. Murphy, *Biochemistry-Moscow* 2005, **70**, 222-230.

13 B. A. Scalettar, J. R. Abney, C. R. Hackenbrock, *P. Natl. Acad. Sci. USA* 1991, **88**, 8057-8061.

14 a) S. Davis, M. J. Weiss, J. R. Wong, T. J. Lampidis, L. B. Chen, *J. Biol. Chem.* 1985, **260**, 3844-3850; b) M. A. Houston, L. H. Augenlicht, B. G. Heerdt, *Plos One* 2011, ***6***, e25207; c) E. H. Shin, Y. Li, U. Kumar, H. V. Sureka, X. R. Zhang, C. K. Payne, *Nanoscale* 2013, **5**, 5879-5886.